A Neutral Cluster Cage with a Tetrahedral [$Pd^{II}_{12}L_6$] Framework: Crystal Structures and Host-Guest Studies

Arvind K. Gupta, Ashok Yadav, Anant Kumar Srivastava, Kormathmadam Raghupathy Ramya, Harshad Paithankar, Shyamapada Nandi, Jeetender Chugh* and Ramamoorthy Boomishankar*

Department of Chemistry, Mendeleev Block, Indian Institute of Science Education and Research, Dr.Homi Bhabha Road, Pune - 411008, India. Fax: +912025908186; E-mail: boomi@iiserpune.ac.in, cjeet@iiserpune.ac.in

Supporting Information

Experimental section and characterization data

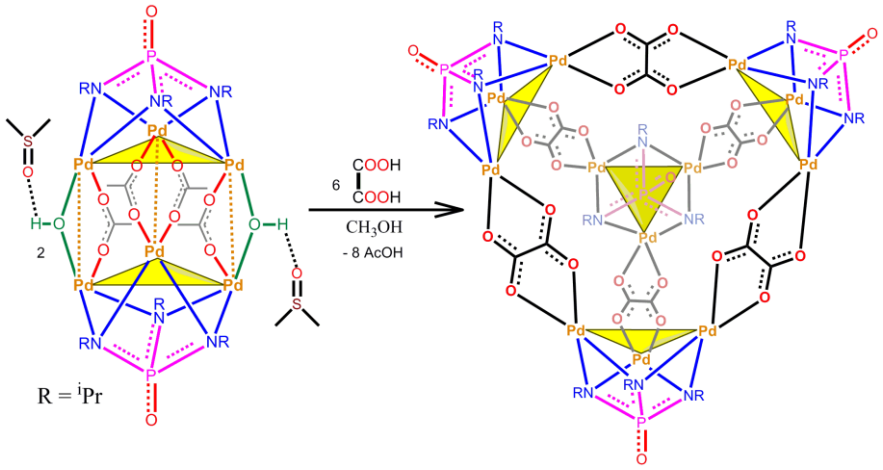

Scheme S1: Synthesis of Tetrahedral cage molecule **2**.

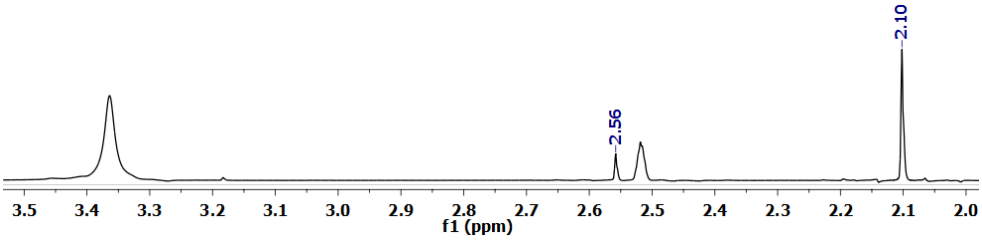

Figure S1: ^{1}H-NMR spectrum of DMSO⊂**2** in d_6-Me_2SO

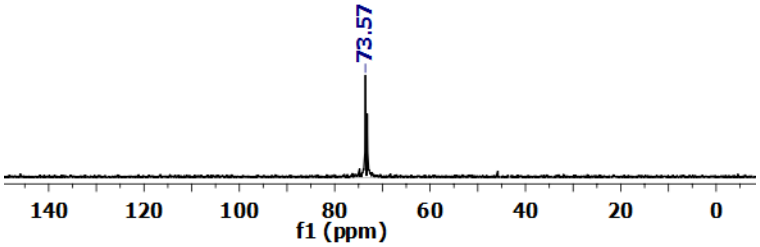

Figure S2: ^{31}P {^{1}H} NMR spectrum of DMSO⊂**2** in d_6-Me_2SO

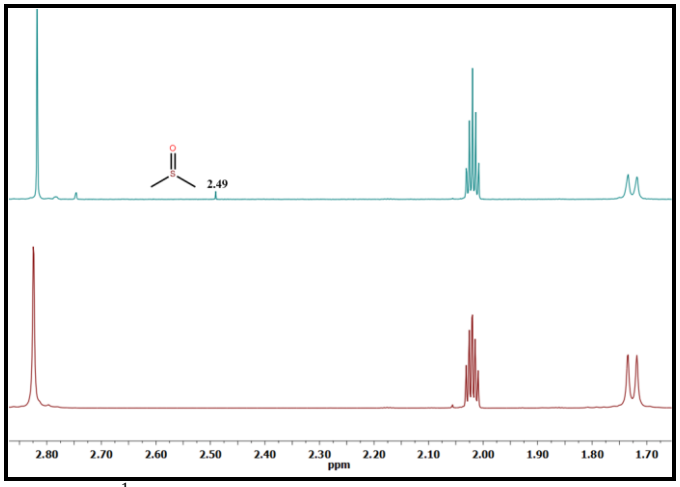

Figure S3: ^{1}H NMR spectra of DMSO⊂**2** and $\mathbf{2}_{\mathbf{free}}$ in d_6-Me_2CO

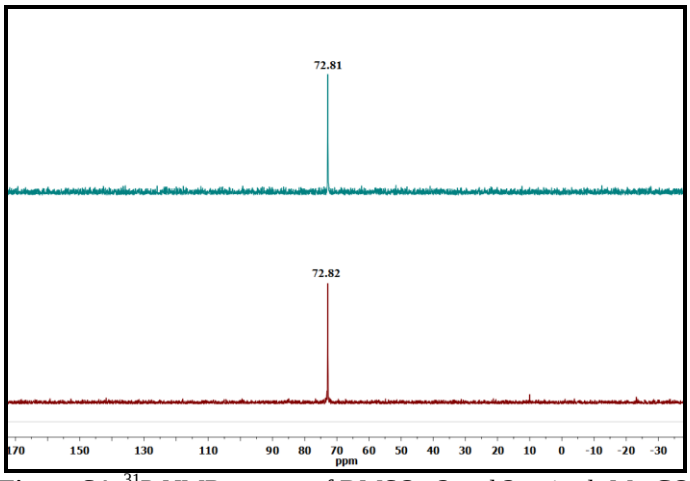

Figure S4: ^{31}P NMR spectra of DMSO⊂**2** and $\mathbf{2}_{\mathbf{free}}$ in d_6-Me_2CO

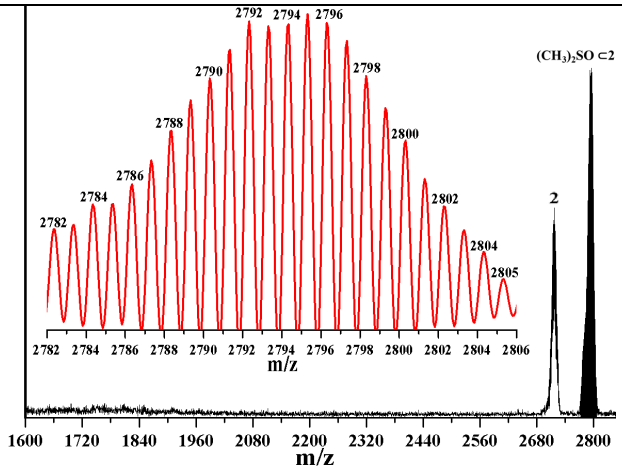

Figure S5: MALDI-TOF Mass spectrum of DMSO⊂**2** in MeOH

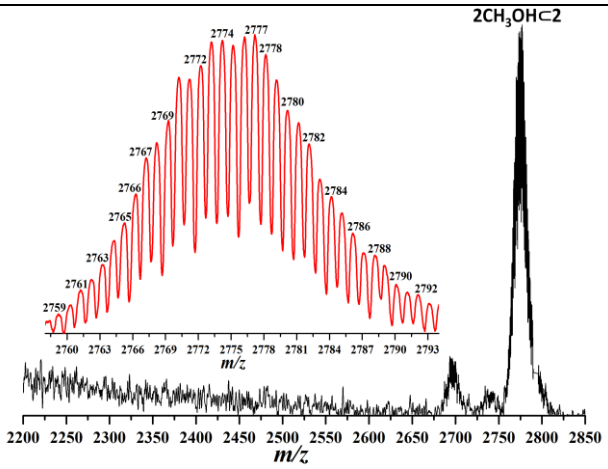

Figure S6: MALDI-TOF Mass spectrum of CH_3OH⊂**2** in MeOH

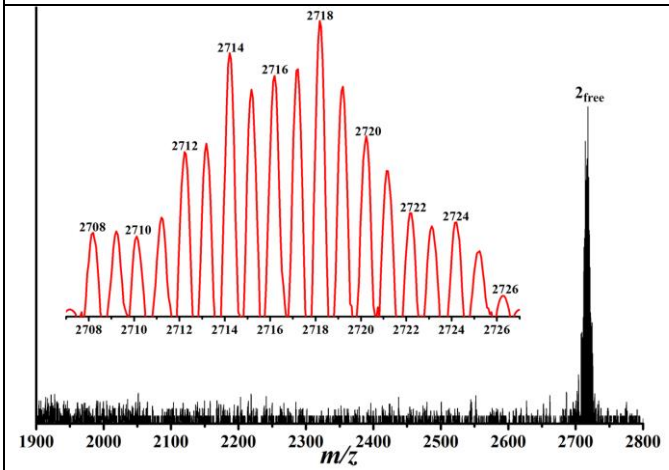

Figure S7: MALDI-TOF Mass spectrum of $\mathbf{2}_{\mathbf{free}}$ in toluene showing only the guest free cage

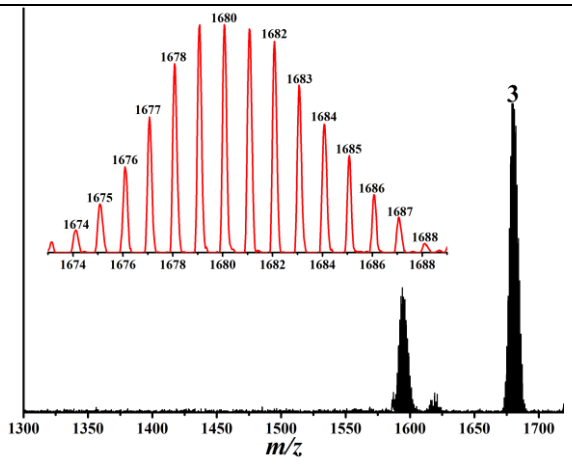

Figure S8: MALDI-TOF Mass spectrum of **3**

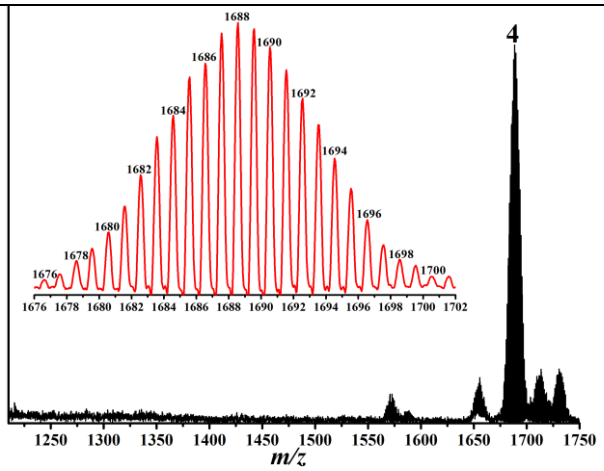

Figure S9: MALDI-TOF Mass spectrum of **4**

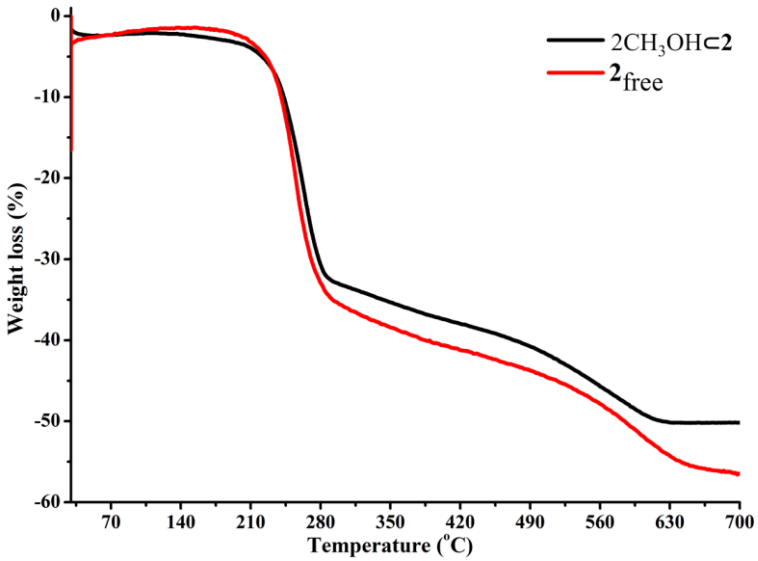

Figure S10: Thermogravimetric (TGA) curves of $2CH_3OH\subset$**2** (black-line) and $\mathbf{2}_{\mathbf{free}}$ (red-line) showing the stability of the sample after desolvation.

Crystallographic data

Table S1: Details of data collection and structure refinements for various Guest⊂**2** complexes

Compound	DMSO⊂**2**	C_6H_6⊂**2**	CCl_4⊂**2**	$CHCl_3$⊂**2**
Chemical formula	$C_{50}H_{90}N_{12}O_{29}P_4Pd_{12}S$	$C_{54}H_{90}N_{12}O_{28}P_4Pd_{12}$	$C_{49}H_{84}N_{12}O_{28}P_4Cl_4P_4d_{12}$	$C_{49}H_{85}N_{12}O_{28}P_4Cl_3Pd_{12}$
Formula weight	2756.54	2756.05	2831.76	2797.32
Temperature K	100(2)	100(2)	100(2)	100(2)
Wavelength Å	0.71073	0.71073	1.54178	0.71073
Crystal system	Orthorhombic	Monoclinic	Monoclinic	Monoclinic
Space group	Cmcm	P2(1)/c	P2(1)/c	P2(1)/n
a (Å); α (°)	18.885(3); 90	17.75(9); 90	18.051(4); 90	17.835(2); 90
b (Å); β(°)	28.732(9); 90	24.00(11); 106.78	23.832(6); 107.46(11)	23.996(3); 107.088(3)
c (Å); γ (°)	24.969(4); 90	29.99(16); 90	29.920(2); 90	29.742(4); 90
V ($Å^3$); Z	13548(4); 4	12239.3(11); 4	12278.7(5); 4	12167(2); 4
ρ (calc.) mg m^{-3}	1.349	1.496	1.532	1.527
μ mm^{-1}	1.662 (Mo K_α)	1.823 (Mo K_α)	15.569 (Cu K_α)	1.899 (Mo K_α)
$2\theta_{max}$ (°)	56	54	136	50
R(int)	0.1953	0.0534	0.0396	0.1335
Completeness to θ	99.7 %	99%	98.7%	99.1%
Data / param.	8919 / 268	26582 / 986	22240 / 1006	21266 / 994
GOF	0.931	0.950	1.079	0.990
R1 [F>4σ(F)]	0.0467	0.0377	0.0415	0.0566
wR2 (all data)	0.1168	0.0956	0.1255	0.155
max. peak/hole (e.$Å^{-3}$)	0.745/ -1.310	1.443 / -1.194	1.385 /-0.650	1.880 / -1.998
Compound	CH_2Cl_2⊂**2**	C_7H_8⊄**2**	C_6H_5Cl⊄**2**	C_6H_5F⊄**2**
Chemical formula	$C_{49}H_{86}N_{12}O_{28}P_4Cl_2Pd_{12}$	$C_{57}H_{98}N_{12}O_{29}P_4SPd_{12}$	$C_{56}H_{95}N_{12}O_{29}P_4SPd_{12}$	$C_{50}H_{90}N_{12}O_{29}P_4SPd_{12}$
Formula weight	2762.88	2848.21	2868.63	2756.07
Temperature K	100(2)	100(2)	100(2)	100(2)
Wavelength Å	0.71073	0.71073	0.71073	0.71073
Crystal system	Monoclinic	Monoclinic	Monoclinic	Monoclinic
Space group	P2(1)/n	P2(1)/c	P2(1)/c	P2(1)/c
a (Å); α (°)	17.78(2); 90	21.477(11); 90	21.447(4); 90	17.780(17); 90
b (Å); β(°)	23.96(3); 107.22(2)	28.389(14); 108.41(2)	28.408(4); 108.562(4)	23.911(2); 107.27(2)
c (Å); γ (°)	29.74(3); 90	17.663(8); 90	17.659(3); 90	29.859(3); 90
V ($Å^3$); Z	12101(2); 4	10218.0(9); 4	10199(3); 4	12137(2); 4
ρ (calc.) mg m^{-3}	1.517	1.851	1.868	1.504
μ mm^{-1}	1.887 (Mo K_α)	2.207 (Mo K_α)	2.237 (Mo K_α)	1.855 (Mo K_α)
$2\theta_{max}$ (°)	56	50	56	56
R(int)	0.1611	0.0930	0.1763	0.1182
Completeness to θ	99.5%	97.4	99.5%	99.7%
Data / param.	29982 / 982	17570 / 1003	25461 / 1050	30249 / 970
GOF	0.823	0.974	0.903	0.921
R1 [F>4σ(F)]	0.0684	0.0452	0.0698	0.0546
wR2 (all data)	0.1807	0.1057	0.1755	0.1291
max. peak/hole (e.$Å^{-3}$)	1.896 / -1.584	1.929 / -1.064	1.461 /-1.566	1.274 /-1.523

Table S2: Details of data collection and structure refinements for **3**·$3H_2O$ and **4**·$3H_2O$

Compound	MeOH⊂**2**	**3**·$3H_2O$	**4**·$3H_2O$
Chemical formula	$C_{98}H_{168}N_{24}O_{58}P_8Pd_{24}$	$C_{60}H_{72}N_6O_{17}P_2Pd_6$	$C_{42}H_{67}N_6O_{15}P_2Pd_6Fe_2$
Formula weight	5411.91	1849.57	1708.05
Temperature K	100(2)	100(2)	100(2)K
Wavelength Å	0.71073	0.71073	0.71073
Crystal system	Triclinic	Monoclinic	Monoclinic
Space group	P-1	P2(1)/c	Cc
a (Å); α (°)	16.838(2); 103.859(3)	14.687(11); 90	20.801(9); 90
b (Å); β(°)	22.889(3); 100.928(3)	21.730(17); 91.768(17)	16.347(8); 122.169(8)
c (Å); γ (°)	22.327(17); 93.835(2)	22.327(17); 90	19.199(12); 90
V ($Å^3$); Z	10500(2); 2	7122(10); 4	5526(5); 4
ρ (calc.) mg m^{-3}	1.712	1.725	2.053
μ mm^{-1}	2.124 (Mo K_α)	1.594 (Mo K_α)	2.540 (Mo K_α)
$2\theta_{max}$ (°)	50.48	50.06	50.06
R(int)	0.1279	0.2169	0.1791
Completeness to θ	97.2%	98.5 %	99.5 %
Data / param.	48392 / 1903	12402 / 489	7909 / 415
GOF	0.824	0.941	0.985
R1 [F>4σ(F)]	0.0654	0.0695	0.0766
wR2 (all data)	0.1543	0.1684	0.1727
max. peak/hole (e.$Å^{-3}$)	1.411 / -1.549	1.006 / -1.205	1.179 / -1.255

Table S3: Selected bond-lengths and angles for DMSO⊂**2**

compound	**Bond lengths**	**Bond Angles**
DMSO⊂**2**	N(1)-P(1): 1.696(7)	P(1)-N(1)-Pd(1)#1: 94.0(2)
	N(1)-Pd(1)#1: 2.021(4)	C(11)-N(1)-Pd(1): 118.0(3)
	N(1)-Pd(1): 2.021(4)	P(1)-N(1)-Pd(1): 94.0(2)
	N(2)-P(1): 1.683(5)	Pd(1)#1-N(1)-Pd(1): 100.7(3)
	N(2)-Pd(2): 2.028(5)	C(21)-N(2)-P(1): 127.2(4)
	N(2)-Pd(1): 2.040(5)	C(21)-N(2)-Pd(2): 117.6(4)
	N(3)-P(2): 1.688(7)	P(1)-N(2)-Pd(2): 93.7(2)
	N(3)-Pd(3)#3: 2.026(4)	C(21)-N(2)-Pd(1): 118.1(4)
	N(3)-Pd(3): 2.026(4)	P(1)-N(2)-Pd(1): 93.7(2)
	N(4)-P(2): 1.684(4)	Pd(2)-N(2)-Pd(1): 100.6(2)
	N(4)-Pd(3): 2.013(5)	C(31)-N(3)-P(2): 125.1(5)
	N(4)-Pd(4): 2.017(4)	C(31)-N(3)-Pd(3)#3: 117.6(3)
	O(1L)-Pd(1): 2.058(4)	P(2)-N(3)-Pd(3)#3: 94.1(2)
	O(2L)-Pd(3): 2.053(4)	C(31)-N(3)-Pd(3): 117.6(3)
	O(3L)-Pd(1): 2.062(4)	P(2)-N(3)-Pd(3): 94.1(2)
	O(4L)-Pd(3): 2.063(4)	Pd(3)#3-N(3)-Pd(3): 103.1(3)
	O(5L)-Pd(4): 2.050(4)	C(41)-N(4)-P(2): 126.4(3)
	O(10)-Pd(2): 2.067(4)	C(41)-N(4)-Pd(3): 118.5(3)
	O(11)-P(1): 1.455(5)	P(2)-N(4)-Pd(3): 94.7(2)
	O(21)-P(2): 1.472(5)	C(41)-N(4)-Pd(4): 117.6(3)
	P(1)-N(2)#1: 1.683(5)	P(2)-N(4)-Pd(4): 94.1(2)
	P(1)-Pd(2): 2.718(2)	Pd(3)-N(4)-Pd(4): 99.56(19)
	P(1)-Pd(1)#1: 2.7275(18)	C(1L)-O(1L)-Pd(1): 111.3(4)
	P(1)-Pd(1): 2.7275(18)	C(1L)-O(2L)-Pd(3): 110.4(3)
	P(2)-N(4)#3: 1.684(4)	C(2L)-O(3L)-Pd(1): 110.4(4)
	P(2)-Pd(4): 2.719(2)	C(2L)-O(4L)-Pd(3): 111.5(4)
	P(2)-Pd(3)#3: 2.7288(18)	C(3L)-O(5L)-Pd(4): 110.7(4)
	P(2)-Pd(3): 2.7289(18)	C(4L)-O(10)-Pd(2): 109.3(4)
	Pd(1)-Pd(1)#1: 3.1119(10)	O(11)-P(1)-N(2): 120.8(2)
	Pd(1)-Pd(2): 3.1298(8)	O(11)-P(1)-N(2)#1: 120.8(2)
	Pd(2)-N(2)#1: 2.028(5)	N(2)-P(1)-N(2)#1: 96.2(3)
	Pd(2)-O(10)#1: 2.067(4)	O(11)-P(1)-N(1): 121.0(3)
	Pd(2)-Pd(1)#1: 3.1298(8)	N(2)-P(1)-N(1): 95.9(2)
	Pd(3)-Pd(4): 3.0773(7)	N(2)#1-P(1)-N(1): 95.9(2)

	Pd(3)-Pd(3)#3: 3.1735(10) Pd(4)-N(4)#3: 2.017(4) Pd(4)-O(5L)#3: 2.050(4) Pd(4)-Pd(3)#3: 3.0773(7)	O(11)-P(1)-Pd(2): 138.5(3) N(2)-P(1)-Pd(2): 48.12(16) N(2)#1-P(1)-Pd(2): 48.12(16) N(1)-P(1)-Pd(2): 100.5(2) O(11)-P(1)-Pd(1)#1: 138.56(14) N(2)-P(1)-Pd(1)#1: 100.60(18) N(2)#1-P(1)-Pd(1)#1: 48.29(17) N(1)-P(1)-Pd(1)#1: 47.66(13) Pd(2)-P(1)-Pd(1)#1: 70.16(5) O(11)-P(1)-Pd(1): 138.56(14) N(2)-P(1)-Pd(1): 48.29(17) N(2)#1-P(1)-Pd(1): 100.60(18) N(1)-P(1)-Pd(1): 47.66(13) Pd(2)-P(1)-Pd(1): 70.16(5) Pd(1)#1-P(1)-Pd(1): 69.57(6) O(21)-P(2)-N(4): 121.7(2) O(21)-P(2)-N(4)#3: 121.7(2) N(4)-P(2)-N(4)#3: 95.4(3) O(21)-P(2)-N(3): 121.2(3) N(4)-P(2)-N(3): 95.0(2) N(4)#3-P(2)-N(3): 95.0(2) O(21)-P(2)-Pd(4): 140.9(2) N(4)-P(2)-Pd(4): 47.71(15) N(4)#3-P(2)-Pd(4): 47.72(15) N(3)-P(2)-Pd(4): 97.9(2) O(21)-P(2)-Pd(3)#3: 137.78(12) N(4)-P(2)-Pd(3)#3: 100.51(17) N(4)#3-P(2)-Pd(3)#3: 47.32(16) N(3)-P(2)-Pd(3)#3: 47.78(13) Pd(4)-P(2)-Pd(3)#3: 68.78(5) O(21)-P(2)-Pd(3): 137.78(12) N(4)-P(2)-Pd(3): 47.32(16) N(4)#3-P(2)-Pd(3): 100.51(17) N(3)-P(2)-Pd(3): 47.78(13) Pd(4)-P(2)-Pd(3): 68.78(5) Pd(3)#3-P(2)-Pd(3): 71.11(6)
3·3H_2O	Pd(1)-O(3): 2.012(8) Pd(1)-N(3): 2.013(10) Pd(1)-N(2): 2.044(8) Pd(1)-O(1): 2.073(7) Pd(1)-P(1): 2.705(3) Pd(2)-N(1): 2.023(8) Pd(2)-N(3): 2.036(9) Pd(2)-O(9): 2.044(8) Pd(2)-O(11L): 2.063(7) Pd(2)-P(1): 2.720(4) Pd(3)-N(2): 2.019(9) Pd(3)-O(5): 2.038(9) Pd(3)-O(7): 2.039(8) Pd(3)-N(1): 2.055(9) Pd(3)-P(1): 2.718(4) Pd(4)-N(5): 2.031(9) Pd(4)-O(6): 2.040(8) Pd(4)-O(8): 2.041(7) Pd(4)-N(4): 2.051(8) Pd(4)-P(2): 2.720(4) Pd(5)-N(4): 2.029(9) Pd(5)-O(2): 2.042(8) Pd(5)-N(6): 2.043(9) Pd(5)-O(4): 2.057(8) Pd(5)-P(2): 2.722(4) Pd(6)-N(5): 1.994(10) Pd(6)-N(6): 2.023(9)	O(3)-Pd(1)-N(3): 167.1(3) O(3)-Pd(1)-N(2): 90.8(3) N(3)-Pd(1)-N(2): 76.7(4) O(3)-Pd(1)-O(1): 97.1(3) N(3)-Pd(1)-O(1): 94.4(3) N(2)-Pd(1)-O(1): 164.0(3) O(3)-Pd(1)-P(1): 128.7(2) N(3)-Pd(1)-P(1): 38.6(3) N(2)-Pd(1)-P(1): 38.3(3) O(1)-Pd(1)-P(1): 130.5(2) N(1)-Pd(2)-N(3): 76.5(3) N(1)-Pd(2)-O(9): 92.8(3) N(3)-Pd(2)-O(9): 163.7(3) N(1)-Pd(2)-O(11L): 169.4(3) N(3)-Pd(2)-O(11L): 95.3(3) O(9)-Pd(2)-O(11L): 93.7(3) N(1)-Pd(2)-P(1): 38.4(2) N(3)-Pd(2)-P(1): 38.4(2) O(9)-Pd(2)-P(1): 128.9(2) O(11L)-Pd(2)-P(1): 132.6(2) N(2)-Pd(3)-O(5): 94.3(4) N(2)-Pd(3)-O(7): 167.3(3) O(5)-Pd(3)-O(7): 95.5(3) N(2)-Pd(3)-N(1): 76.3(4) O(5)-Pd(3)-N(1): 164.7(3) O(7)-Pd(3)-N(1): 92.3(3) N(2)-Pd(3)-P(1): 38.0(3)

	Pd(6)-O(12): 2.046(9) Pd(6)-O(10): 2.052(7) Pd(6)-P(2): 2.726(4) P(1)-O(11): 1.485(7) P(1)-N(2): 1.678(10) P(1)-N(3): 1.691(9) P(1)-N(1): 1.691(9) P(2)-O(21): 1.463(7) P(2)-N(6): 1.695(10) P(2)-N(4): 1.711(10) P(2)-N(5): 1.719(9)	O(5)-Pd(3)-P(1): 130.4(2) O(7)-Pd(3)-P(1): 130.1(2) N(1)-Pd(3)-P(1): 38.4(2) N(5)-Pd(4)-O(6): 169.2(3) N(5)-Pd(4)-O(8): 94.2(3) O(6)-Pd(4)-O(8): 94.6(3) N(5)-Pd(4)-N(4): 77.9(4) O(6)-Pd(4)-N(4): 92.0(3) O(8)-Pd(4)-N(4): 163.9(3) N(5)-Pd(4)-P(2): 39.2(2) O(6)-Pd(4)-P(2): 130.4(2) O(8)-Pd(4)-P(2): 130.7(2) N(4)-Pd(4)-P(2): 39.0(3) N(4)-Pd(5)-O(2): 167.7(3) N(4)-Pd(5)-N(6): 77.1(4) O(2)-Pd(5)-N(6): 93.7(4) N(4)-Pd(5)-O(4): 91.4(3) O(2)-Pd(5)-O(4): 96.0(3) N(6)-Pd(5)-O(4): 164.6(3) N(4)-Pd(5)-P(2): 38.9(3) O(2)-Pd(5)-P(2): 130.9(2) N(6)-Pd(5)-P(2): 38.5(3) O(4)-Pd(5)-P(2): 128.6(2) N(5)-Pd(6)-N(6): 77.0(4) N(5)-Pd(6)-O(12): 163.2(3) N(6)-Pd(6)-O(12): 96.1(4) N(5)-Pd(6)-O(10): 91.1(3) N(6)-Pd(6)-O(10): 167.4(4) O(12)-Pd(6)-O(10): 94.2(3) N(5)-Pd(6)-P(2): 39.0(2) N(6)-Pd(6)-P(2): 38.3(3) O(12)-Pd(6)-P(2): 131.2(2) O(10)-Pd(6)-P(2): 129.3(3) O(11)-P(1)-N(2): 120.2(5) O(11)-P(1)-N(3): 120.4(5) N(2)-P(1)-N(3): 96.7(4) O(11)-P(1)-N(1): 121.1(5) N(2)-P(1)-N(1): 96.7(5) N(3)-P(1)-N(1): 95.9(4) O(11)-P(1)-Pd(1): 135.2(4) O(21)-P(2)-N(6): 121.6(5) O(21)-P(2)-N(4): 120.5(5) N(6)-P(2)-N(4): 96.4(5) O(21)-P(2)-N(5): 121.0(5)
4·$3H_2O$	Pd(1)-N(1): 2.028(18) Pd(1)-O(6): 2.054(15) Pd(1)-N(3): 2.055(17) Pd(1)-O(9): 2.058(15) Pd(1)-P(1): 2.739(7) Pd(1)-Pd(6): 3.056(3) Pd(1)-Pd(3): 3.098(3) Pd(2)-N(2): 2.041(18) Pd(2)-O(10): 2.050(15) Pd(2)-N(3): 2.060(18) Pd(2)-O(4): 2.076(15) Pd(2)-P(1): 2.732(7) Pd(2)-Pd(4): 3.040(3) Pd(2)-Pd(3): 3.064(3) Pd(3)-N(2): 2.013(16) Pd(3)-O(2): 2.024(15) Pd(3)-N(1): 2.037(18) Pd(3)-O(8): 2.058(13) Pd(3)-P(1): 2.719(6)	N(1)-Pd(1)-O(6): 90.1(6) N(1)-Pd(1)-N(3): 75.8(7) O(6)-Pd(1)-N(3): 163.5(6) N(1)-Pd(1)-O(9): 173.1(7) O(6)-Pd(1)-O(9): 91.8(6) N(3)-Pd(1)-O(9): 103.1(7) N(2)-Pd(2)-O(10): 170.8(7) N(2)-Pd(2)-N(3): 76.2(7) O(10)-Pd(2)-N(3): 99.4(7) N(2)-Pd(2)-O(4): 91.1(6) O(10)-Pd(2)-O(4): 94.5(6) N(3)-Pd(2)-O(4): 163.9(6) N(2)-Pd(3)-O(2): 92.6(7) N(2)-Pd(3)-N(1): 76.3(7) O(2)-Pd(3)-N(1): 167.7(6) N(2)-Pd(3)-O(8): 167.5(7) O(2)-Pd(3)-O(8): 97.1(6) N(1)-Pd(3)-O(8): 93.2(6) O(10)-Pd(4)-N(5): 96.4(7)

	Pd(4)-O(10): 2.032(16) Pd(4)-N(5): 2.043(19) Pd(4)-N(4): 2.044(17) Pd(4)-O(3): 2.052(16) Pd(4)-P(2): 2.708(7) Pd(4)-Pd(5): 3.095(3) Pd(5)-O(7): 2.020(13) Pd(5)-N(6): 2.027(18) Pd(5)-N(4): 2.049(17) Pd(5)-O(1): 2.053(14) Pd(5)-P(2): 2.727(5) Pd(5)-Pd(6): 3.106(3) Pd(6)-N(6): 2.02(2) Pd(6)-N(5): 2.029(17) Pd(6)-O(5): 2.039(15) Pd(6)-O(9): 2.058(16) Pd(6)-P(2): 2.726(7) P(1)-O(11): 1.467(16) P(1)-N(1): 1.685(17) P(1)-N(2): 1.687(19) P(1)-N(3): 1.698(19) P(2)-O(21): 1.450(15) P(2)-N(4): 1.678(19) P(2)-N(6): 1.679(18) P(2)-N(5): 1.76(2) Fe(1)-C(3L): 2.03(2) Fe(1)-C(12L): 2.03(2) Fe(1)-C(6L): 2.04(2) Fe(1)-C(2L): 2.04(2) Fe(1)-C(11L): 2.04(2) Fe(1)-C(5L): 2.05(2) Fe(1)-C(8L): 2.05(2) Fe(1)-C(4L): 2.06(2) Fe(1)-C(10L): 2.06(2) Fe(1)-C(9L): 2.09(2) Fe(2)-C(21L): 2.01(2) Fe(2)-C(17L): 2.02(2) Fe(2)-C(15L): 2.02(2) Fe(2)-C(16L): 2.03(2) Fe(2)-C(24L): 2.03(2) Fe(2)-C(23L): 2.04(2) Fe(2)-C(22L): 2.04(2) Fe(2)-C(14L): 2.04(2) Fe(2)-C(18L): 2.05(2) Fe(2)-C(20L): 2.06(2) O(1)-C(1L): 1.27(2) O(2)-C(1L): 1.26(2) O(3)-C(7L): 1.23(2) O(4)-C(7L): 1.25(3) O(5)-C(13L): 1.24(2) O(6)-C(13L): 1.23(3) O(7)-C(19L): 1.28(2) O(8)-C(19L): 1.24(2)	O(10)-Pd(4)-N(4): 173.2(7) N(5)-Pd(4)-N(4): 78.4(8) O(10)-Pd(4)-O(3): 95.3(6) N(5)-Pd(4)-O(3): 166.7(7) N(4)-Pd(4)-O(3): 90.4(7) O(7)-Pd(5)-N(6): 94.3(6) O(7)-Pd(5)-N(4): 167.7(6) N(6)-Pd(5)-N(4): 75.6(7) O(7)-Pd(5)-O(1): 95.3(5) N(6)-Pd(5)-O(1): 168.5(7) N(4)-Pd(5)-O(1): 94.1(6) N(6)-Pd(6)-N(5): 77.7(8) N(6)-Pd(6)-O(5): 91.9(7) N(5)-Pd(6)-O(5): 167.5(7) N(6)-Pd(6)-O(9): 173.7(8) N(5)-Pd(6)-O(9): 97.6(7) O(5)-Pd(6)-O(9): 93.3(6) Pd(1)-O(9)-Pd(6): 95.9(6) Pd(4)-O(10)-Pd(2): 96.3(6) O(11)-P(1)-N(1): 120.9(10) O(11)-P(1)-N(2): 121.4(10) N(1)-P(1)-N(2): 95.8(9) O(11)-P(1)-N(3): 120.1(9) N(1)-P(1)-N(3): 95.7(9) N(2)-P(1)-N(3): 96.7(9) O(11)-P(1)-Pd(3): 143.9(8) N(1)-P(1)-Pd(3): 48.4(6) N(2)-P(1)-Pd(3): 47.6(6) N(3)-P(1)-Pd(3): 96.0(6) P(1)-N(1)-Pd(1): 94.6(8) P(1)-N(1)-Pd(3): 93.3(9) Pd(1)-N(1)-Pd(3): 99.3(7) P(1)-N(2)-Pd(3): 94.2(8) P(1)-N(2)-Pd(2): 93.7(8) Pd(3)-N(2)-Pd(2): 98.2(7) P(1)-N(3)-Pd(1): 93.2(8) P(1)-N(3)-Pd(2): 92.7(8) Pd(1)-N(3)-Pd(2): 109.5(7) O(21)-P(2)-N(4): 120.0(10) O(21)-P(2)-N(6): 122.0(10) N(4)-P(2)-N(6): 96.2(9) O(21)-P(2)-N(5): 120.1(9) N(4)-P(2)-N(5): 97.5(9) N(6)-P(2)-N(5): 95.2(10) P(2)-N(4)-Pd(4): 92.8(8) P(2)-N(4)-Pd(5): 93.5(10) Pd(4)-N(4)-Pd(5): 98.3(7) P(2)-N(5)-Pd(6): 91.8(9) P(2)-N(5)-Pd(4): 90.6(8) Pd(6)-N(5)-Pd(4): 111.1(7) P(2)-N(6)-Pd(6): 94.6(9) P(2)-N(6)-Pd(5): 94.3(10) Pd(6)-N(6)-Pd(5): 100.4(8) C(1L)-O(1)-Pd(5): 136.8(14) C(1L)-O(2)-Pd(3): 141.1(14) C(7L)-O(3)-Pd(4): 128.1(15) C(7L)-O(4)-Pd(2): 126.0(14) C(13L)-O(5)-Pd(6): 126.2(14) C(13L)-O(6)-Pd(1): 126.7(14) C(19L)-O(7)-Pd(5): 134.2(14) C(19L)-O(8)-Pd(3): 137.8(14) O(2)-C(1L)-O(1): 125(2) O(2)-C(1L)-C(2L): 116.3(19)

		O(1)-C(1L)-C(2L): 118.5(19) C(6L)-C(5L)-C(4L): 108(2) C(6L)-C(5L)-Fe(1): 69.8(13) O(3)-C(7L)-O(4): 128(2) O(3)-C(7L)-C(8L): 117(2) O(4)-C(7L)-C(8L): 115(2) O(6)-C(13L)-O(5): 130(2) O(6)-C(13L)-C(14L): 112.1(19) O(5)-C(13L)-C(14L): 118(2)

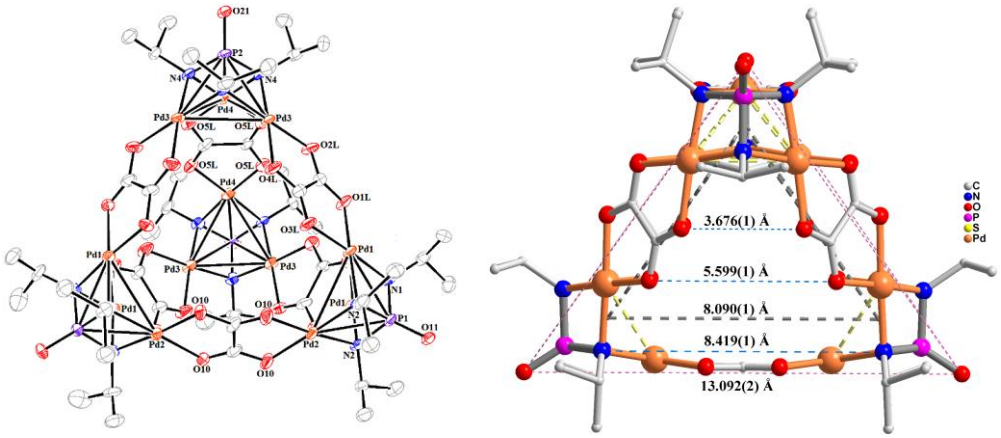

a **b**

Figure S11: (a) Ortep diagram of the core structure of **2** at 50% ellipsoid probability. Hydrogen atoms and encapsulated DMSO are omitted for clarity. The metric parameters associated with Pd-Pd, Pd-O and Pd-N bonds in the $[Pd_3X]^{3+}$ PBU are closely matching with those found in **1**.2DMSO (average Pd-Pd = 3.123(1) Å, Pd-N = 2.024(5) Å, Pd-O = 2.058(4) Å and P-N = 1.688(5) Å); (b) view of the various portal, edge and central distances measured in the crystal structure of **2**. The average Pd-Pd distances within the triangular Pd_3-unit is 3.123(1) Å and is matching closely with those observed in **1**.2DMSO.

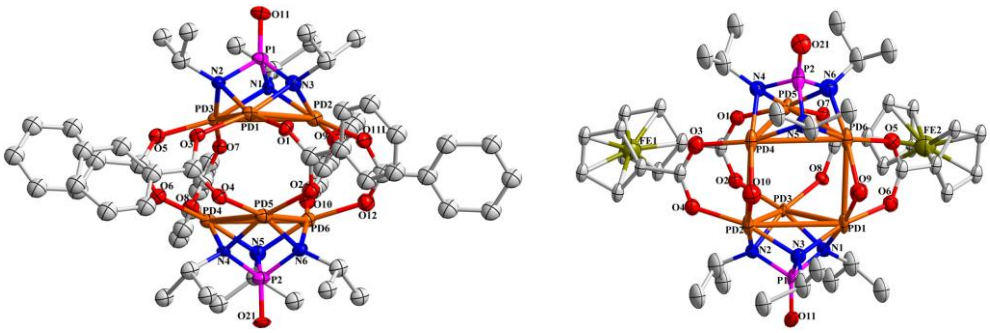

a **b**

Figure S12: Ortep diagram of (a) **3** and (b) **4** at 50% ellipsoid probability**.**

Cavity Volume Calculations

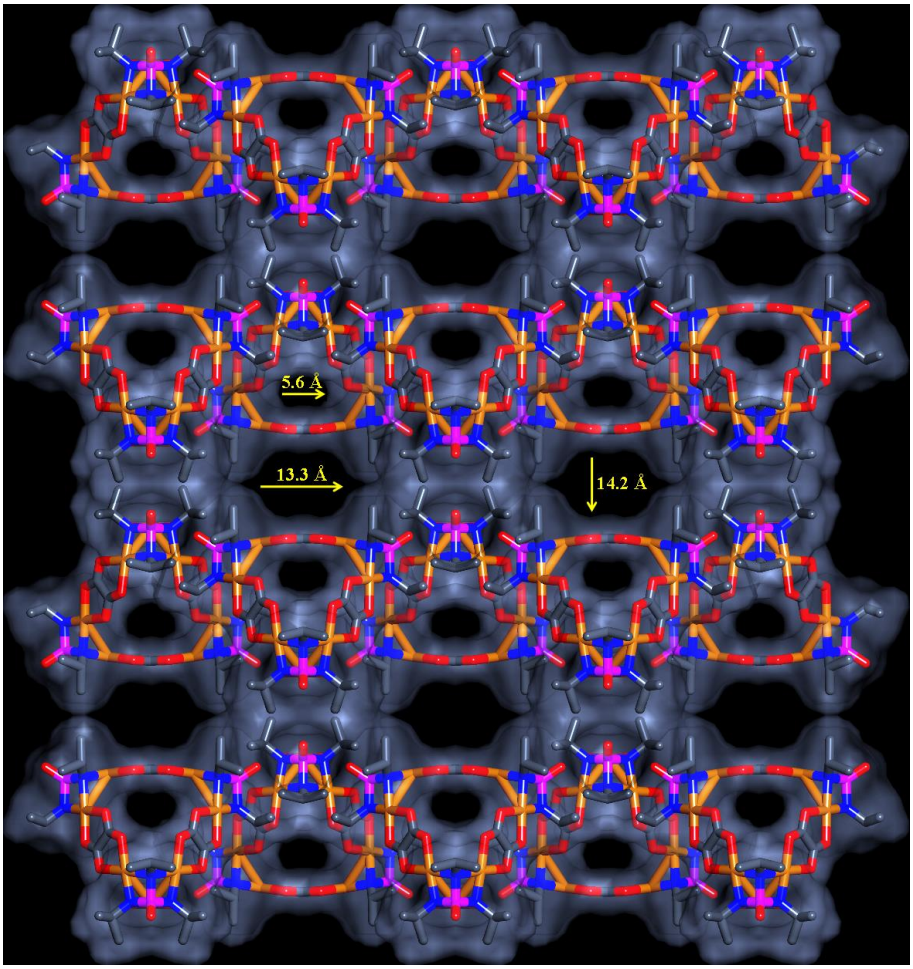

Figure S13: Surface overlay view of the 2x2x2 packing structure of **2** along the c-axis showing the presence of two distinct types of voids.

Table S4: Volume and area calculated for intrinsic cavity of **2** from MSROLL calculations[a]

Probe Radius (Å)	Surface Area (Å^2)	Volume (Å^3)
1.27	102.094	86.963
1.28	101.666	86.580
1.29	101.248	86.205
1.3	100.841	85.835
1.4	97.225	82.420
1.5	94.142	79.337

[a]The probe escapes from the cavity upon lowering the radius below 1.27 Å. As the cavity of the cage is fairly small with narrow portal dimensions the probe radius for the discussions was fixed at 1.3 Å

Gas Sorption Analysis

From the adsorption profile it is evident that CO_2 exhibits a higher uptake capacity of 3.4 mmol/g at 195K compared to N_2 (2.4 mmol/g at 77K) and H_2 (1.9 mmol/g at 77K) (Figure S13-S15 SI). The better CO_2 uptake can be attributed to its effective interactions with the polar oxalate bridges in **2**. The BET and Langmuir surface areas in **2** based on its 195K CO_2 uptake profile are calculated to be 293.24 (correlation coefficient = 0.9998) and 459.58 (correlation coefficient=0.9999) m^2/g, respectively. Further, based on the 263, 273 and 298 K adsorption data, the isosteric heat of adsorption (Q_{st}) for CO_2 in **2** was calculated to be 37 kJ/mol (Figures S16-S17).

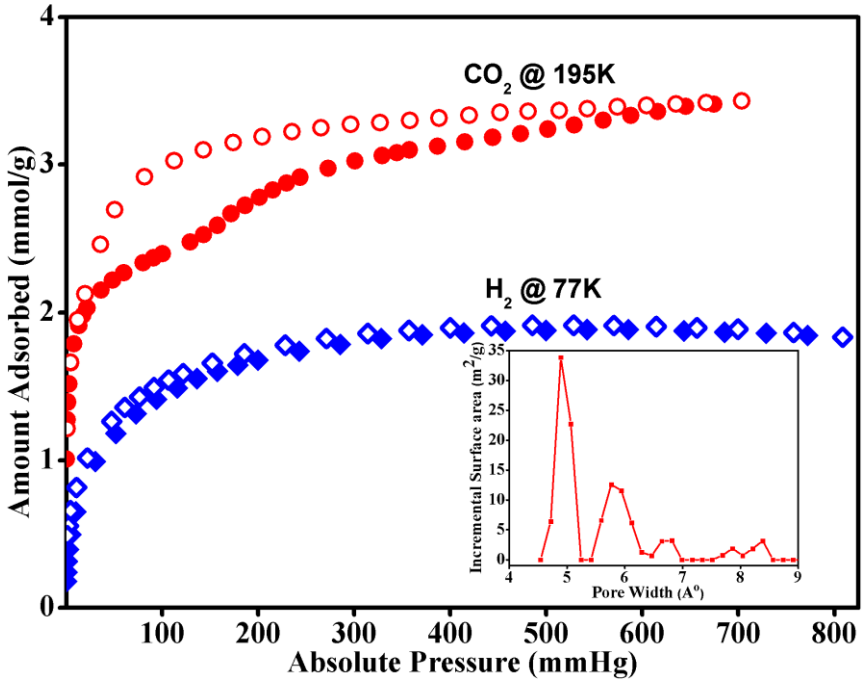

Figure S14. Red: CO_2 adsorption at 195K and Blue: H_2 adsorption at 77K. Open symbols represent desorption. Inset: pore size distribution in **2** calculated from 195K CO_2 data.

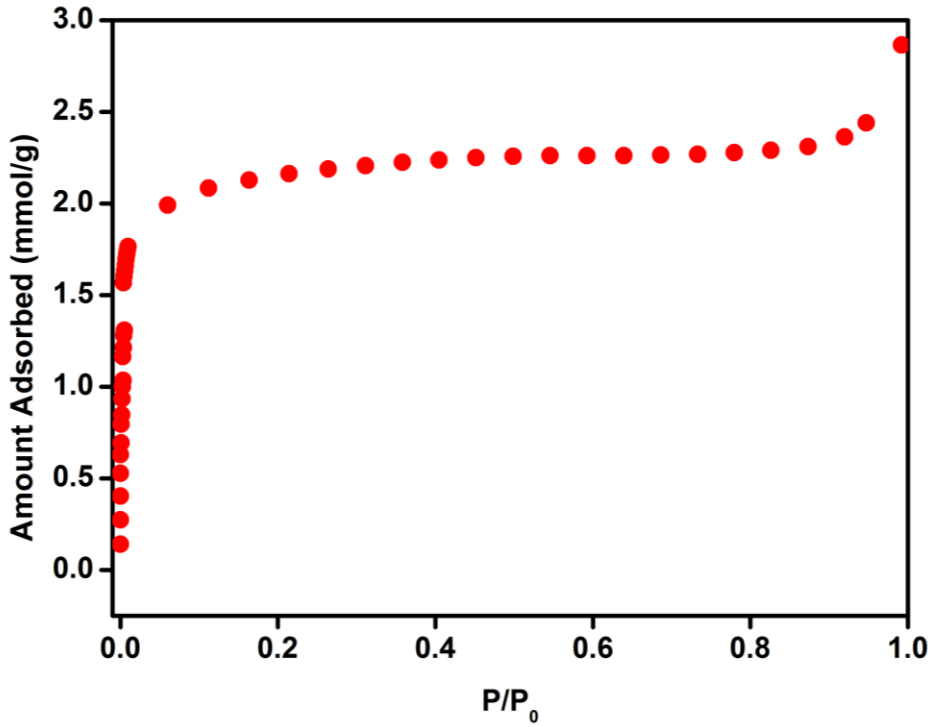

Figure S15: N_2 adsorption at 77K. Note: Desorption branch has not been shown as it was too slow.

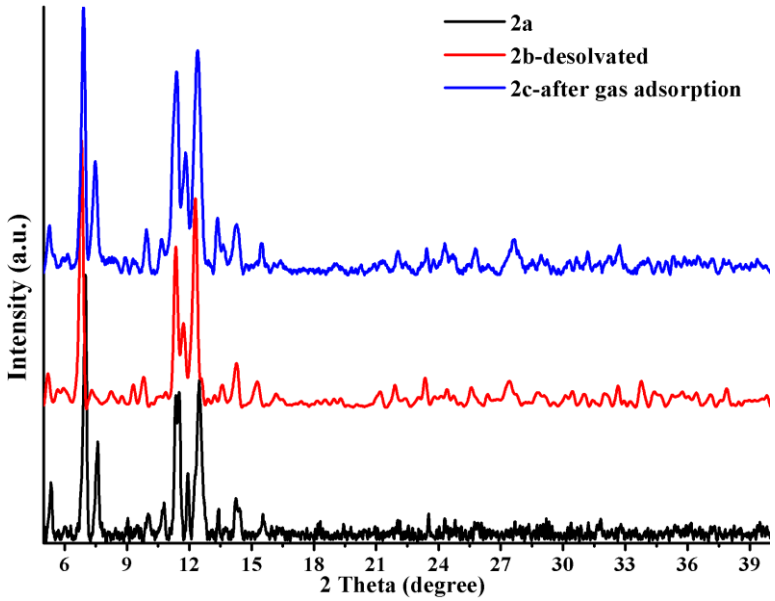

Figure S16: The PXRD patterns for the various samples of **2** showing the crystallinity and structural stability after gas adsorption.

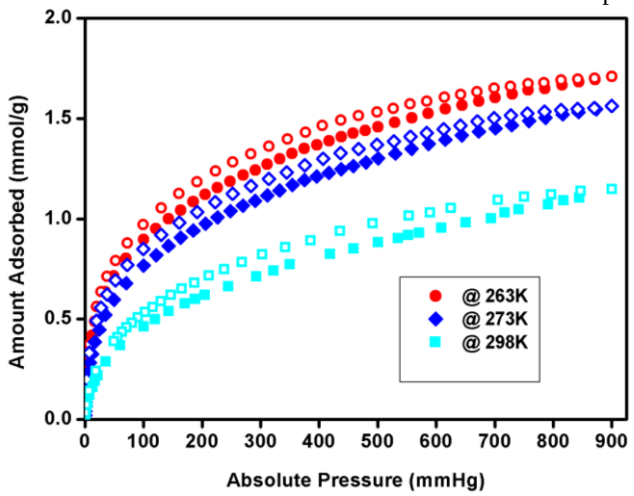

Figure S17: CO_2 isotherms at three different temperatures. The open symbols in all cases represent desorption.

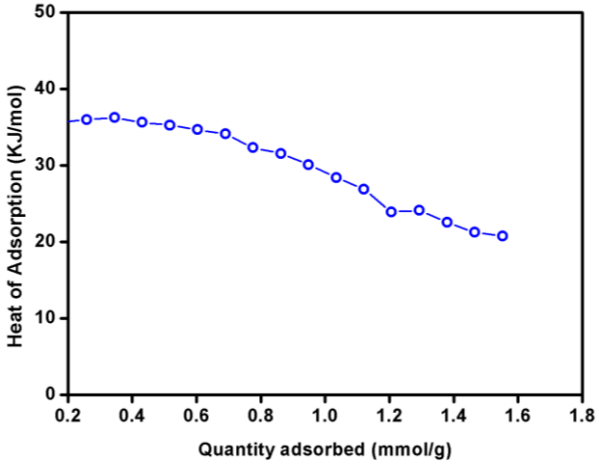

Figure S18: Heat of adsorption (Q_{st}) vs loading graph for CO_2 at **2**. Q_{st} for CO_2 adsorption on the cluster calculated from 263, 273, 298 K isotherms using DFT modelling.

Guest Encapsulation Studies

Table S5: List of guest molecules screened for encapsulation within the host structure of **2** and the corresponding observations

Guest	Surface Area [Å^2]	Molecular Volume [Å^3]	Encapsulation observed for cage 2	Crystal structure
CH_2Cl_2	83.62	60.83	Yes	Yes
$CHCl_3$	99.58	74.68	Yes	Yes
DMSO	96.3	76.40	Yes	Yes
CCl_4	115.38	88.69	Yes	Yes
Benzene	114.95	99.16	Yes	Yes
Cyclopentane	98.3	70.7	Yes	No
Flurobenzene	120.77	103.83	No	Yes
Cyclohexane	129.29	111.48	No	No
Chlorobenzene	143.58	129.00	No	Yes
Toluene	149.16	134.77	No	Yes

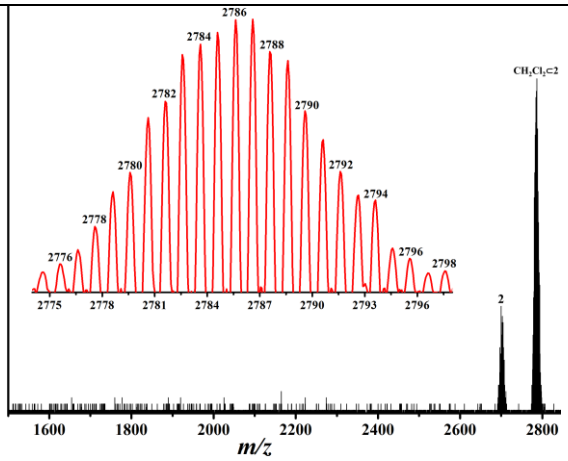

Figure S19: MALDI-TOF Mass spectrum of CH_2Cl_2⊂**2**

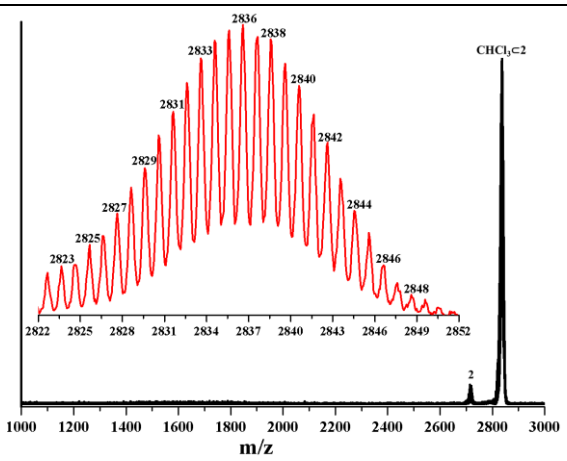

Figure S20: MALDI-TOF Mass spectrum of $CHCl_3$⊂**2**

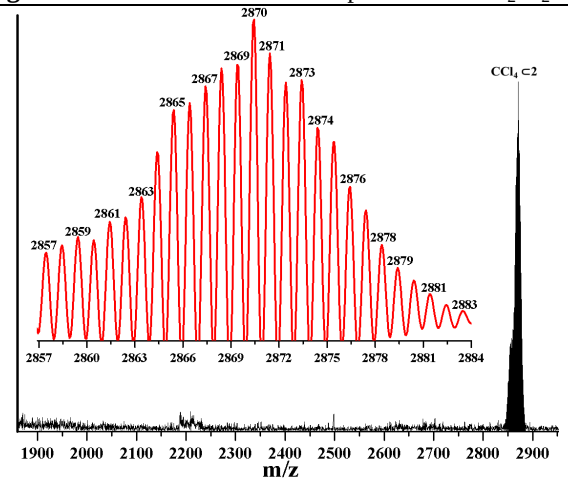

Figure S21: MALDI-TOF Mass spectrum of CCl_4⊂**2**

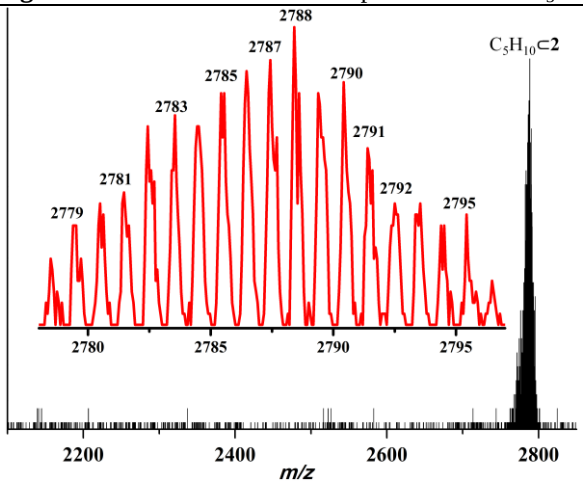

Figure S22: MALDI-TOF Mass spectrum of C_5H_{10}⊂**2**

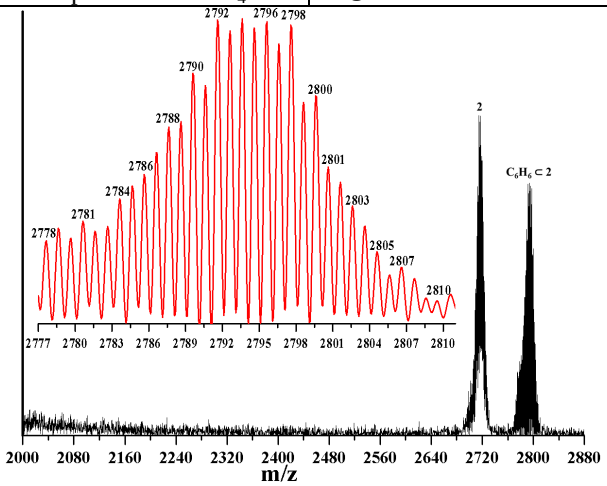

Figure S23: MALDI-TOF Mass spectrum of C_6H_6⊂**2**

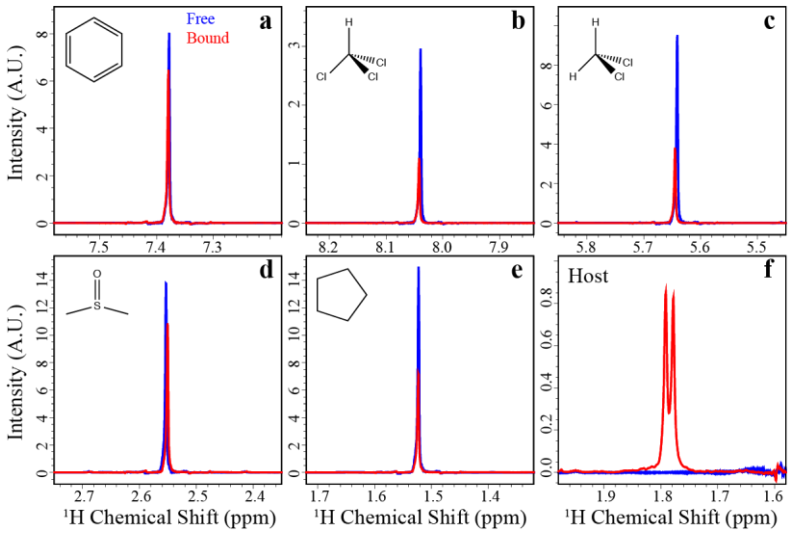

Figure S24: Overlay of ^{1}H NMR spectrum of (a) benzene, (b) chloroform, (c) dichloromethane, (d) DMSO, (e) cycopentane in the absence (blue) and presence (red) of host highlighting overlap of free and bound signals; (f) ^{1}H NMR spectrum of host protons highlighting absence (blue) and presence (red) of host.

Table S6: Diffusion coefficients as obtained from the DOSY experiment for host and different guests in the studied host-guest systems

Solvent	Diffusion Coefficient ($1*E^{-11}$ m^2/s)			
	Host		**Guest**	
	Free	Bound	Free	Bound
C_6H_6	92.47	16.6	416	3.86
$CHCl_3$	94.47	11.51	366.4	20.51
CH_2Cl_2	92.67	9.957	454.3	30.29
DMSO	95.94	10.46	417.5	26.22
C_5H_{10}	92.96	6.038	440.5	15.93

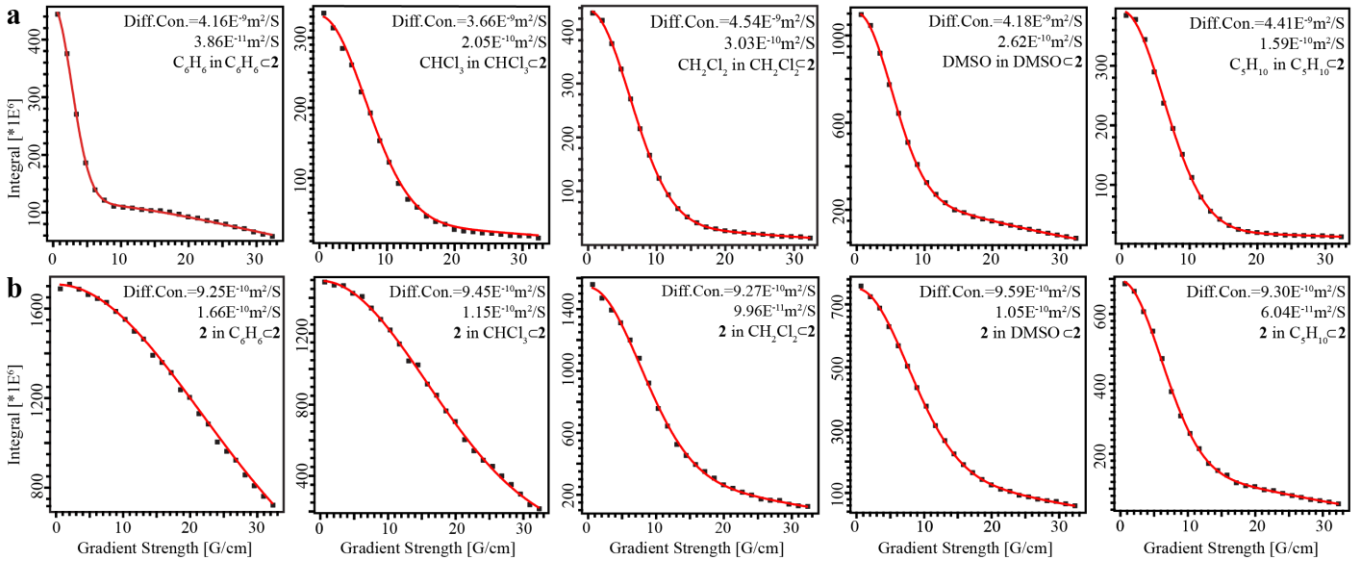

Figure S25: Integral decay profile of (a) guest protons in the host-guest system, (b) host protons in the host-guest system plotted as a function of gradient strength. The dots represent experimental data and the red line shows the best fit using the equation 1. Name of the guest molecule and the diffusion coefficients obtained for free and bound molecule are shown in the corresponding insets.

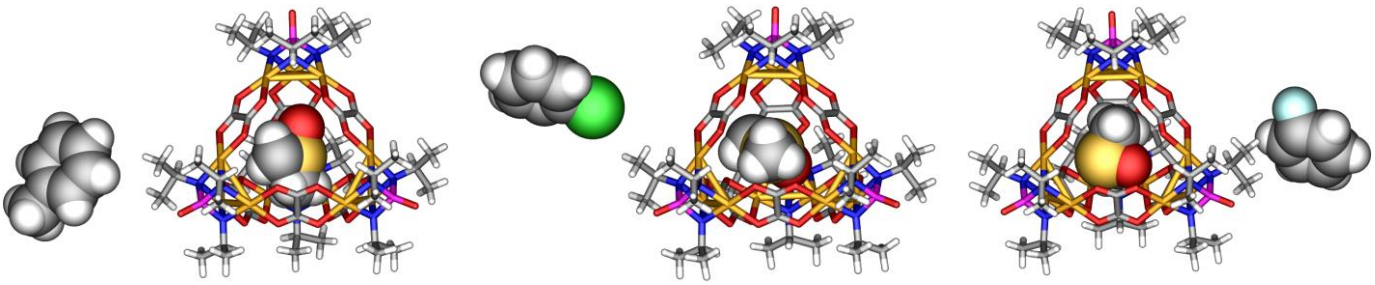

a **b** **c**

Figure S26: Molecular structures of (a) C_7H_8⊄**2** (b) C_6H_5Cl⊄**2** (c) C_6H_5F⊄**2** with the encapsulated DMSO

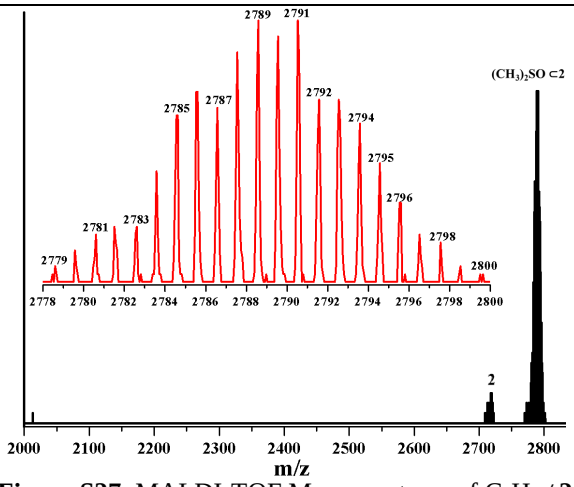

Figure S27: MALDI-TOF Mass spectrum of C_7H_8⊄**2**

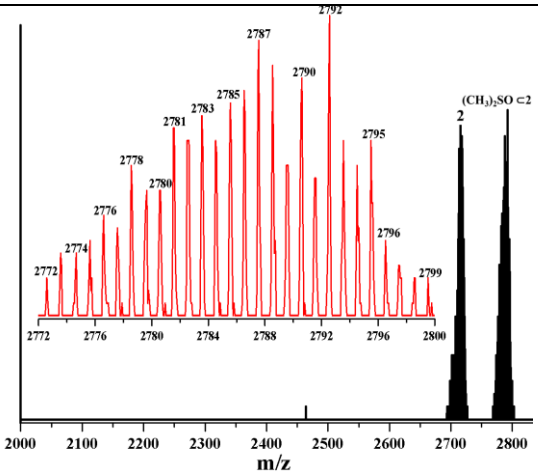

Figure S28: MALDI-TOF Mass spectrum of C_6H_5F⊄**2**

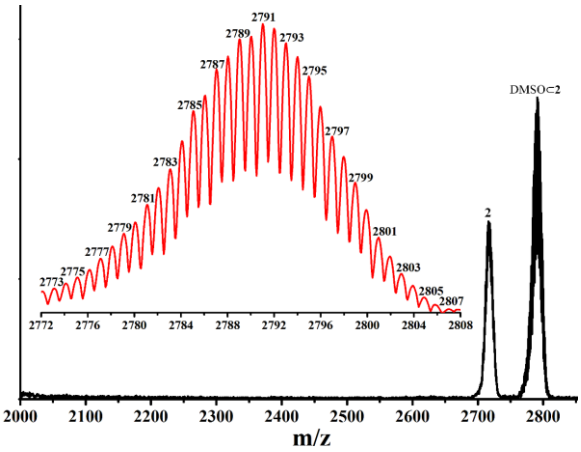

Figure S29: MALDI-TOF Mass spectra of C_6H_5Cl⊄**2**

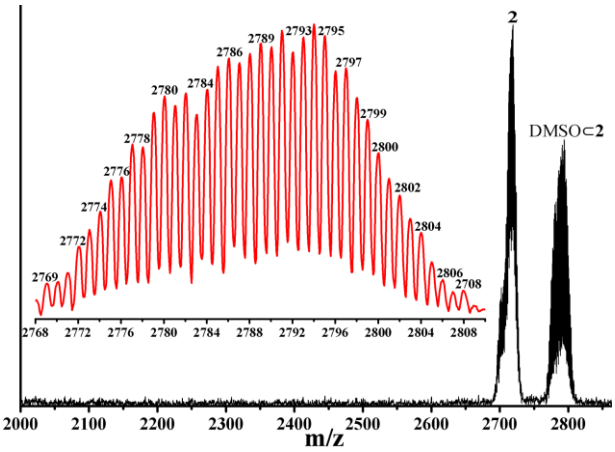

Figure S30: MALDI-TOF Mass spectrum of C_6H_{12}⊄**2**

Selective Guest Encapsulation Studies: To a stirred mixture of equal amounts (0.5 mL) of C_6H_6, CCl_4 CH_2Cl_2, $CHCl_3$ and THF, 1.2DMSO (10 mg, 0.007 mmol) was added. The final solution was stirred for one hour and concentrated to about 0.5 mL under vacuum. The resulting mixture was diluted in methanol and analyzed by MALDI-TOF mass spectroscopy which revealed the formation of C_6H_6⊂**2** at m/z = 2795. Single crystals suitable for X-ray analysis was obtained by slow evaporation from a methanolic solution of this mixture. Initial X-ray analysis performed on these crystals reveal the presence of C_6H_6⊂**2** (four different crystals were screened with the same cell parameters and initial structure solution). ^{1}H-NMR spectrum of these crystals also reveal the presence of benzene at δ = 7.32 ppm. Similar experiment with only chlorinated solvents revealed the presence of CCl_4⊂**2** as observed from mass spectrum (m/z = 2870) and by single crystal x-ray analysis on crystals obtained from the diluted methanolic solution of the mixture. The same observations were made when exchange experiments were performed separately on CH_2Cl_2⊂**2** and $CHCl_3$⊂**2** with benzene and CCl_4 (Figure S31).

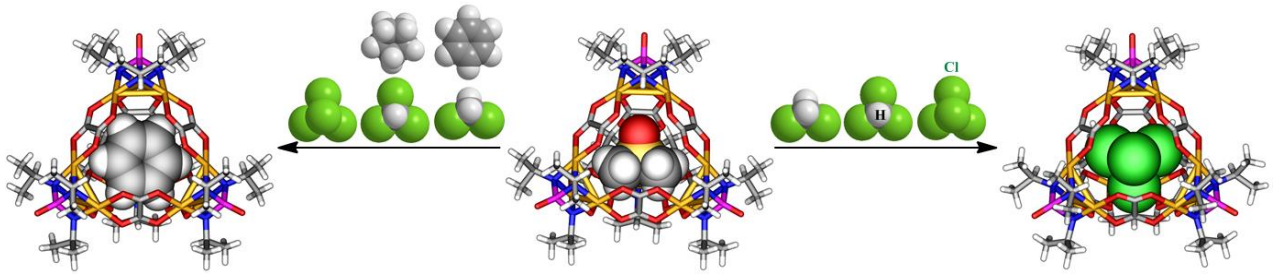

Figure S31: Selective Guest Encapsulation Studies

Stability Studies

Thermogravimetric Analysis: The TGA graphs of all these solvent encapsulated assemblies show that an initial weight loss of about 10 % was observed for most solvents below 200 °C and in all these cases the onset of cage decomposition is observed around 240 °C.

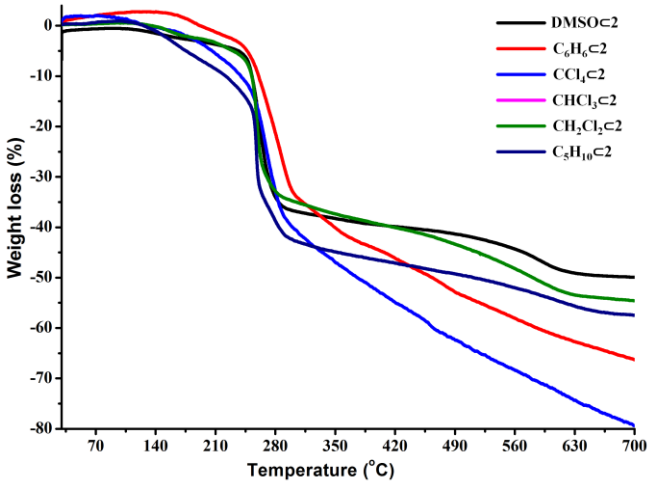

Figure S32: Thermogravimetric (TGA) curves of $CHCl_3$⊂**2**, CH_2Cl_2⊂**2**, CCl_4⊂**2** C_6H_6⊂**2** and C_5H_{10}⊂**2**

pH Dependant Stability Studies: In a typical pH stability experiment 1 mg (0.0004 mmol) of DMSO⊂**2** was stirred with 0.5 mL of a buffer solution and 0.5 mL of acetone for 10-12 hours at 50°C. The resultant solution was subjected to mass spectral analysis. The MALDI-TOF mass spectra of DMSO⊂**2** treated with various pH buffer solutions is given in the figure S29. From the mass spectral analysis it is evident that the tetrahedral cage assembly of **2** was intact in the pH range between 3.5 and 9. However at pH 3.5 the concentration of the cage was very low as observed from very weak mass spectral signatures in the cage region. In fact no cage peak was observed for buffer solutions below pH 3.5. To further validate these observations we took ^{31}P-NMR spectra of these samples at slightly higher concentrations. For this purpose 3 mg (0.0012 mmol) of DMSO⊂**2** was stirred with 0.35 mL of a buffer solution and 0.4 mL of acetone for 10-12 hours at 50°C. The ^{31}P-NMR (with external $CDCl_3$ locking) reveal that the peak due to the $[Pd_3X]^{3+}$ PBU was retained in the pH range between 4.5 and 9. However, this peak was absent for the sample treated with the pH = 3.5 solution (Figure S30). These experiments suggest that the cage structure is retained for a wide pH range and could be useful for encapsulation and controlled release of guest molecules. Spectral studies on samples treated with pH > 9 buffer solutions could not be performed due to poor solubility of the cage assembly in these solutions. The buffer solutions were prepared in 10 mL quantities in 200 mM concentrations as below.
The buffer solutions of pH between 3.5 and 9.0 were prepared by mixing the appropriate quantities of 200 mM aqueous solutions of NaH_2PO_4 or Na_2HPO_4 and adjusting the pH by a drop wise addition of 1 M aqueous solutions of H_3PO_4 or NaOH monitored by the pH meter.

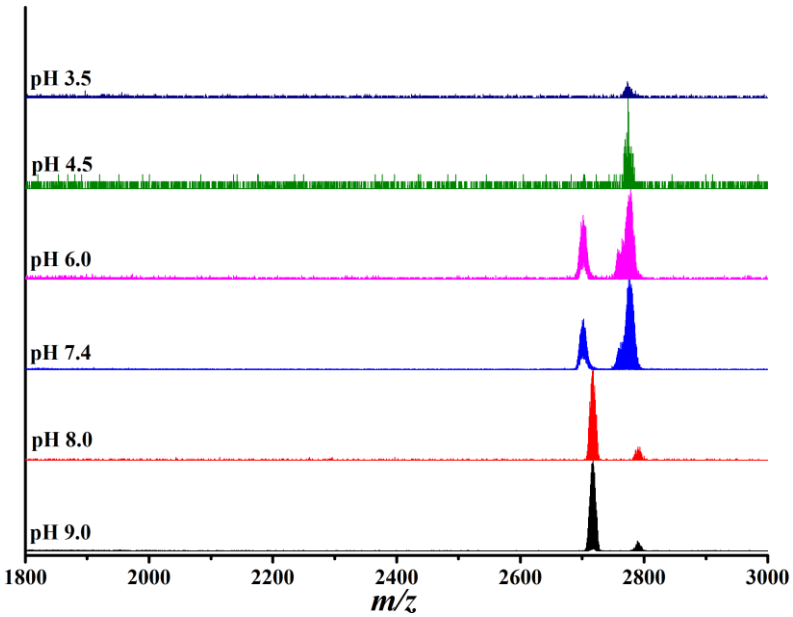

Figure S33: MALDI-TOF Mass spectra for DMSO⊂**2** in various pH buffer solutions showing the isotopic distribution of peaks due to **2** and/or DMSO⊂**2**.

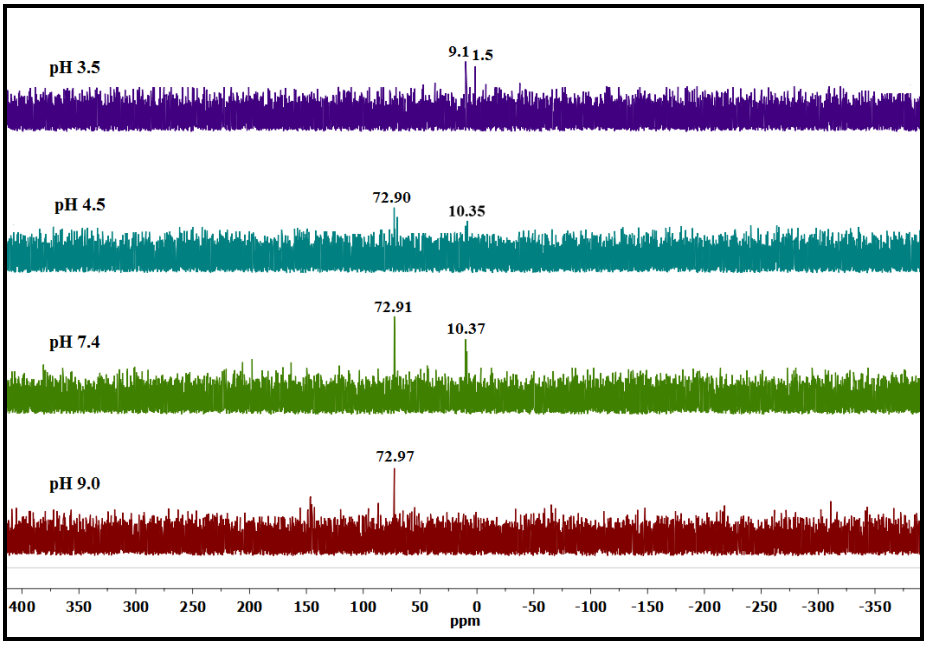

Figure S34: ^{31}P-NMR spectra for DMSO⊂**2** in various pH buffer solutions showing the signal due to the trianionic imido-phosphate trianion in the PBU segments around δ = 72.9 ppm (external $CDCl_3$ locking). The noisy baseline is due to the lower concentrations of **2** in the buffer solutions.

Preferential Formation of the Tetrahedral Cage under Competitive Conditions:

In order to see the formation of the cage assembly of **2** in presence of an indirect oxalate source, we treated 1.2DMSO with $Fe_2(C_2O_4)_3 \cdot 6H_2O$. Thus to a stirred solution of 1.2DMSO (10 mg, 0.007 mmol) in methanol (2 mL) and iron (III) oxalate hexa-hydrate (4 mg, 0.013 mmol) in methanol (2 mL) was added and the resulting mixture was heated for 30 min at 80 ^{o}C. Then the solvents were evaporated to dryness to yield a crude sample. The MALDI-TOF mass spectrum of this sample showed the formation of DMSO⊂**2** along with ferric acetate $\{Fe_3O(OAc)_6(H_2O)_3]OAc\}$.[1] Further confirmation was obtained from SC-XRD when this crude sample was crystallized from methanol/DMSO mixtures which gave the same structural parameter as that of DMSO⊂**2**·10DMSO·$5H_2O$. Formation of the Pd-oxalate coordination against the Fe-oxalate bonds in this occasion demonstrates a remarkable stability for the cage structure of **2** (Scheme S2 and Figure S35, supporting information).

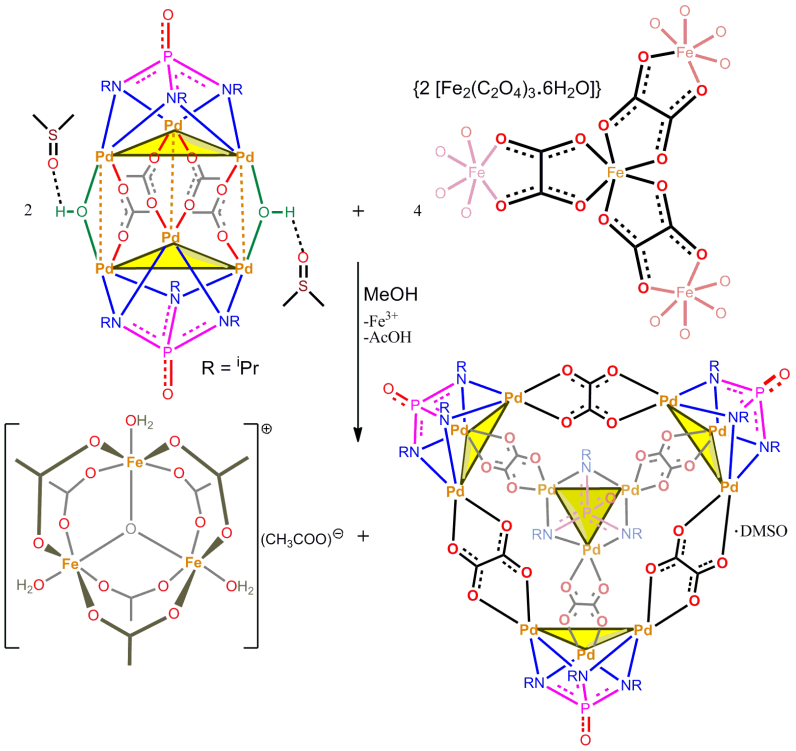

Scheme S2: Synthesis of the tetrahedral cage assembly of DMSO⊂**2** from an indirect oxalate source

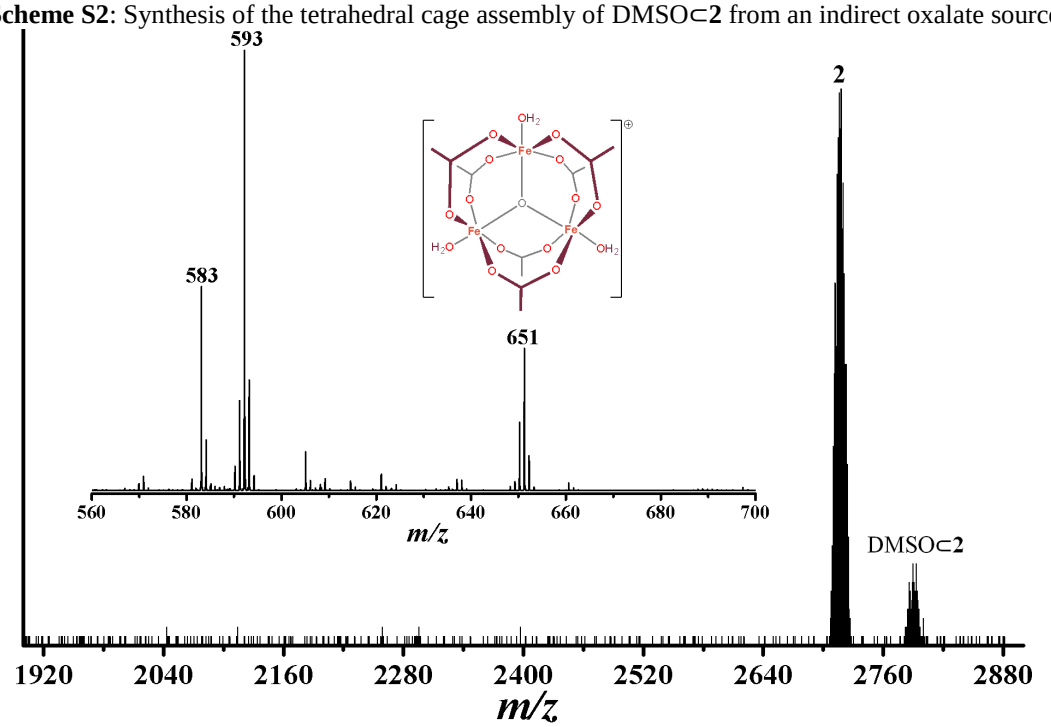

Figure S35: MALDI-TOF Mass spectrum of the reaction mixture of **1**.2DMSO, oxalic acid and $Fe_2(C_2O_4)_3{\cdot}6H_2O$ in methanol. Inset shows the partial mass spectrum of the sample in the m/z region between 500 and 700 showing the formation of ferric oxalate minor product $\{Fe_3O(OAc)_6(H_2O)_3]OAc\}$. The m/z centered at 651 corresponds to the cation $\{Fe_3O(OAc)_6(H_2O)_3]\}^+$ and m/z centered at 593 corresponds to the species $[Fe_3O(OAc)_6]^+$.

References

1. (a) Cotton, F. A. Advanced Inorganic Chemistry, *Wiley, New York,* **1980**, 154-155. (b) Catterick, J.; Thornton, P. *Adv. Inorg. Chem. Radiochem.* **1977**, *20*, 291-362. (c) Cannon R. D.; White, R. P. *Prog. Inorg. Chem.* **1988**, *36*, 195-298.